

Article

# Eco-Approach and Departure System for Left-Turn Vehicles at a Fixed-Time Signalized Intersection

Huifu Jiang , Shi An, Jian Wang \* and Jianxun Cui

School of Transportation Science and Engineering, Harbin Institute of Technology, Harbin 150001, China; 13B932001@hit.edu.cn (H.J.); anshi@hit.edu.cn (S.A.); cuijianxun@hit.edu.cn (J.C.)

\* Correspondence: wang\_jian@hit.edu.cn

Received: 3 December 2017; Accepted: 18 January 2018; Published: 22 January 2018

**Abstract:** This research proposed an eco-approach and departure system for left-turn vehicles at a fixed-time signalized intersection. This system gives higher priority to enhancing traffic safety than improving mobility and fuel efficiency, and optimizes the entire traffic consisted of connected and automated vehicles (CAVs) and conventional human-driven vehicles by providing ecological speed trajectories for left-turn CAVs. All the ecological speed trajectories are offline optimized before the implementation of system. The speed trajectory optimization is constructed in Pontryagin's Minimum Principle structure. The before and after evaluation of the proposed system shows the percentage of vehicles that drive pass the intersection at safe speed increases by 2.14% to 45.65%, fuel consumption benefits range 0.53% to 18.44%, emission benefits range from 0.57% to 15.69%, no significant throughput benefits is observed. The proposed system significantly enhances the traffic safety and improves the fuel efficiency and emission reduction of left-turn vehicles with no adverse effect on mobility, and has a good robustness against the randomness of traffic. The investigation also indicates that the computation time of proposed system is greatly reduced compared to previous eco-driving system with online speed optimization. The computation time is up to 0.01 s. The proposed system is ready for real-time application.

**Keywords:** eco-approach and departure; left-turn vehicles; fixed-time signalized intersection; traffic safety; mobility; fuel efficiency and emissions reduction; offline optimization

## 1. Introduction

Due to that the transportation is one of the major sources in greenhouse gas emissions [1], how to improve the fuel efficiency and reduce emissions has become a focus of research [2]. Many researchers have conducted a number of studies on it from different perspective, including green driving behaviors [3–6], ecological clean energies and power technologies [7,8], advanced traffic control [9,10] and vehicle control [11]. With the development of emerging communication and control technologies, eco-driving control which attempts to smooth the speed profile vehicles promptly became a hotspot of research. The relevant researches can be categorized into eco-driving on freeway [9,10,12–14] and on signalized arterial [14–20]. Eco-driving on freeway mainly focuses on reducing the vehicles' velocity oscillation when they are following a leading vehicle. Eco-driving on signalized arterial mainly studies on reducing the vehicles' acceleration, deceleration and idling maneuvers as they travel through a signalized corridor.

Many eco-driving control methods on signalized arterial have been proposed in the existing studies. Saboohi designed an eco-driving strategy which can reduce the fuel consumption by optimizing the speed and gear ratio of vehicles [21]. Mandava developed an arterial velocity planning algorithms which could minimize the acceleration/deceleration rates to reduce the fuel consumption and emissions of individual vehicle [15]. Later, Barth proposed an upgraded algorithm with the

minimum objective function of tractive power requirements of individual vehicle which shows a much better performance than before [16,22–26]. Kamal used the model predictive control for improve vehicle's ecology in varying traffic environment [27]. Rakha designed an eco-driving framework that has detailed microscope fuel consumption and emission model in the objective function [28]. Mensing utilized the dynamic programming approach to optimize the speed trajectories of vehicles [29]. Nunzio adopted graph discretizing approach to identify the ecological spatial-temporal trajectories of vehicles [30]. Madruga applied the multi-agent system to eco-driving training [31]. Some others focused on improving the fuel efficiency of HEV, PHEV or EV at the signalized intersections [8,32]. These methods only get traffic signal information from infrastructure and ignore the impacts of surrounding traffic. To overcome this shortcoming, Liu and Rakha developed two optimal controllers which take the impacts of front queue at the intersection into consideration [33,34]. Since these methods only concerned about the fuel and emissions saving of individual vehicle without considering its impact on following vehicles, they would have a poor ecological performance under heavy traffic and even negative effect on mobility. Thus, Li proposed a parsimonious shooting heuristic algorithm to force all connected and automated vehicles (CAVs) drive pass the intersection with the smallest headway with its preceding vehicle and run at posted speed limit to maximize both throughput and fuel saving [18,19]. Based on this idea, Jiang designed a similar system that is able to function under partially connected and automated vehicles environment by utilizing the impacts of connected and automated vehicles on conventional human-driven vehicles. This system shows a good performance under low market penetration of connected and automated vehicles and good robustness for traffic randomness, and is feasible for implementation in the near future [35].

All the aforementioned studies could provide ecological trajectories for straight-going vehicles. Some other studies attempted to optimize the trajectories of turning vehicles. Lee and Park proposed a control strategy to minimize the length of overlapped trajectories in no signal control intersection zone to help straight-going, left-turning and right-turning vehicles safely pass the intersection without colliding with other vehicles [17]. Rakha designed a simulation/optimization tool to force vehicles drive pass the intersection at a desired speed which is based on the turning maneuver [36]. Similarly, Huang adopted sequential convex optimization method to construct an optimal controller with the constraint of turning motion [37]. Compared with the eco-driving methods for straight-going vehicles, the key point of methods for turning vehicles is ensuring the vehicle speed at the intersection in safe ranges. The controllers force vehicles adjust their speed to a value lower than the turning speed limit before reaching the intersection, and end the eco-driving control after they have passed the intersection.

To guarantee the feasible of real-time implementation, most existing studies tried to reduce the computation time of optimization. Barth and Xia simplified the optimization by modelling the acceleration and deceleration stage as trigonometric functions travel time to the intersection [16–22]. Rakha utilized simulation to generate various speed trajectories which comply with the constraints of signal control and then selected the trajectory with lowest fuel consumption as output [36]. Liu decomposed the original multi-stage optimal control problem into a sequence of optimal control sub-problems approximated by optimization models which contains few control variables [33]. Li designed a SH-based optimization framework to check the performance of feasible trajectory vector and output the vector when it is optimal [18]. These simplifications aim at avoiding the infinite dimension optimization problem with nonlinear objective and constraints to reduce the computation time. The simplified methods can only generate approximate optimal speed trajectories to reduce the fuel consumption, but cannot minimize it. To obtain the optimal speed trajectories with less computation time so as to minimize the fuel consumption, Wang, Hu and Jiang constructed the optimization problem in Pontryagin's Minimum Principle structure and use a bi-directional iteration approach to accelerate the solving stage. The computation time in these studies was reduced to  $10^{-1} \sim 10^1$  s, which means these methods can potentially be used in real-time control on connected and automated vehicles with low control frequency ( $\leq 10$  Hz) [8,12,13,35].

The existing eco-driving methods have limitations. First, only a few studies have been made on eco-driving control for turning vehicles, and these limited studies only care about the vehicles' motion on the approaches of intersection, but fail to help the vehicles ecologically depart the intersection with low fuel consumption and emissions. However, relevant researches indicate that eco-departure significantly contribute to fuel saving and emissions reduction of vehicles on signalized arterials [38,39]. Second, the computation time of optimizations in most existing researches is not lower than 0.1 s, the computation speed is still not fast enough for future real-time control on vehicles with high control frequency ( $\geq 10$  Hz). With the development of autonomous driving technologies, the control frequency of automated vehicles will rise further in the coming years [40]. The computation time at  $10^{-1}$  s level will fail to meet the requirement of high control frequency vehicles. Long computation time would cause huge deviations between optimal speed profile generated by optimization and actual speed profile in real traffic and lead to a reduction on the performance of eco-driving control or even traffic safety problem [39]. To make the eco-driving control to be used in future real time application, its computation time should be reduced to less than  $10^{-1}$  s [40].

As described before, the eco-approach control system proposed by Jiang and Hu could control the straight-going traffic under partially connected and automated vehicles environmental, and can generate optimal speed trajectories within a relative short computation time [35]. This system is more feasible for implementation in the near future and has potential to be improved to control the turning vehicles in real time. Therefore, the objective of this study is to improve this eco-approach system into an eco-approach and departure controller that can:

- control the longitudinal motions of left-turn connected and automated vehicles during approaching and departing the intersection
- prioritize safety before maintaining optimal mobility status and improving fuel efficiency (force vehicles drive pass the intersection at a safe turning speed)
- further shorten the computation time of optimal speed trajectory (be fast enough for real-time implementation in the future)

The reminder of the paper is organized as follows: Section 2 'control structure' briefly describes the control structure and highlights of the eco-approach and departure controller; Section 3 'Mathematical Formulation' provides the detailed formulations of computation and optimization problems; Section 4 'Simulation and Evaluation' presents the simulation construction and all results. Section 5 'Conclusion and Future Researches' gives the conclusions and brings up some suggestions for future research.

## 2. Control Structure

The goal of this eco-approach and departure system is to enhance the traffic safety for left-turn vehicles and improve their fuel efficiency and emissions reduction during approaching and departing the signalized intersection while maintaining the mobility. There are four highlights of this controller:

- *Eco-approach and departure*: The controller is installed at the intersection, and provides ecological speed trajectories for the approaching and departing CAVs in the control zone. Each ecological speed trajectory is the most fuel efficiency among all the speed trajectories that satisfy the optimal safety and mobility constraints.
- *Higher safety and mobility priority*: The controller puts a higher priority on safety and mobility than ecology. Due to the left-turn maneuver, the CAVs need to enter the intersection at a safety speed that is much lower than the posted speed limit on the road, which means the CAVs need to adjust their speed to a safety value before reaching the stop bar. The controller enforces the final state of eco-approach stage to ensure the safe turning speed at the stop bar while maximizing the throughput. All CAVs are forced to pass through the intersection with the smallest headway with their preceding vehicles and travel at maximum safe turning speed. These tightest and fastest platoons could maximize the throughput since the flow rate is equal to the product of density and speed.

- *Indirectly control the conventional human-drive vehicle:* The controller optimizes the speed trajectories of the CAVs to optimize the entire traffic flow consisted of CAVs and conventional human-driven vehicles. Due to the car-following behavior of conventional vehicle, the controller could indirectly control the conventional vehicles by utilizing the impact of the CAVs on them.
- *Offline optimization:* The controller pre-generates various optimal eco-approach and departure speed trajectories and stores them in the database. Once a CAV reaches, the controller would query a feasible eco-approach speed trajectory and a feasible eco-departure speed trajectory for it based on its initial state, surrounding traffic and signal control. The time cost of query is much lower than real-time optimization. This design ensures the fast computation speed for real-time implementation.

The eco-approach and departure system for left-turn vehicles requires the following equipment: (1) one vehicle detector installed on the left-turn approach of the intersection which detects the vehicle arrival and collects the initial information of vehicles; (2) communication devices installed on the CAVs and infrastructure which is responsible for the communication between them. The assumptions are as follows:

- No lane-changing and overtaking maneuvers are allowed during the whole eco-approach and departure stage;
- No communication issues are considered, all the CAVs in the control zone could instantly communicate with the controller.

The architecture and control structure of this eco-approach and departure system for left-turn vehicles are presented in Figures 1 and 2 respectively. The system is activated by the vehicle arrival detected by the loop detector. Then the controller attempts to establish communication with the vehicle. Only the CAV would respond to the communication request from the controller. If the vehicle is a CAV, module 2 will be activated. Otherwise, module 1 will be activated. The details of modules in the system are provided in the following:

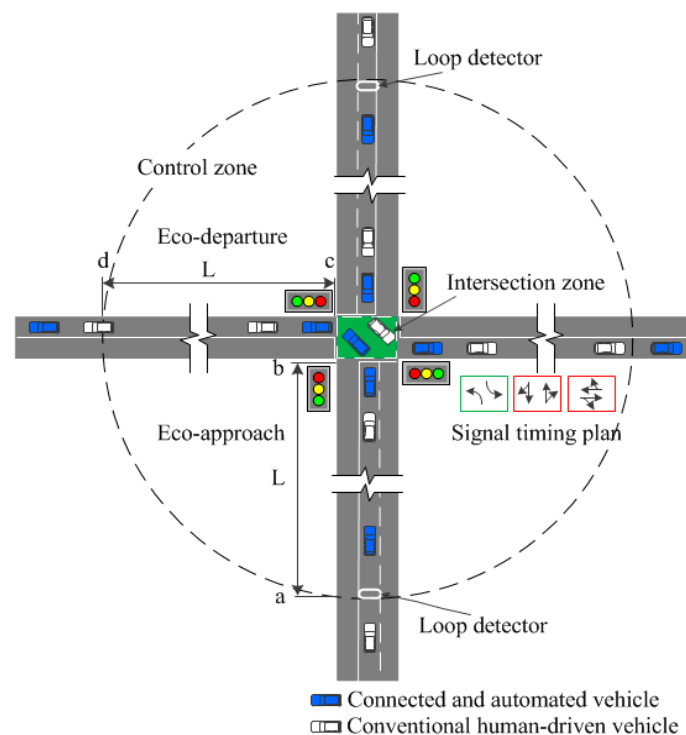


**Figure 1.** Illustration of the eco-approach and departure system architecture.

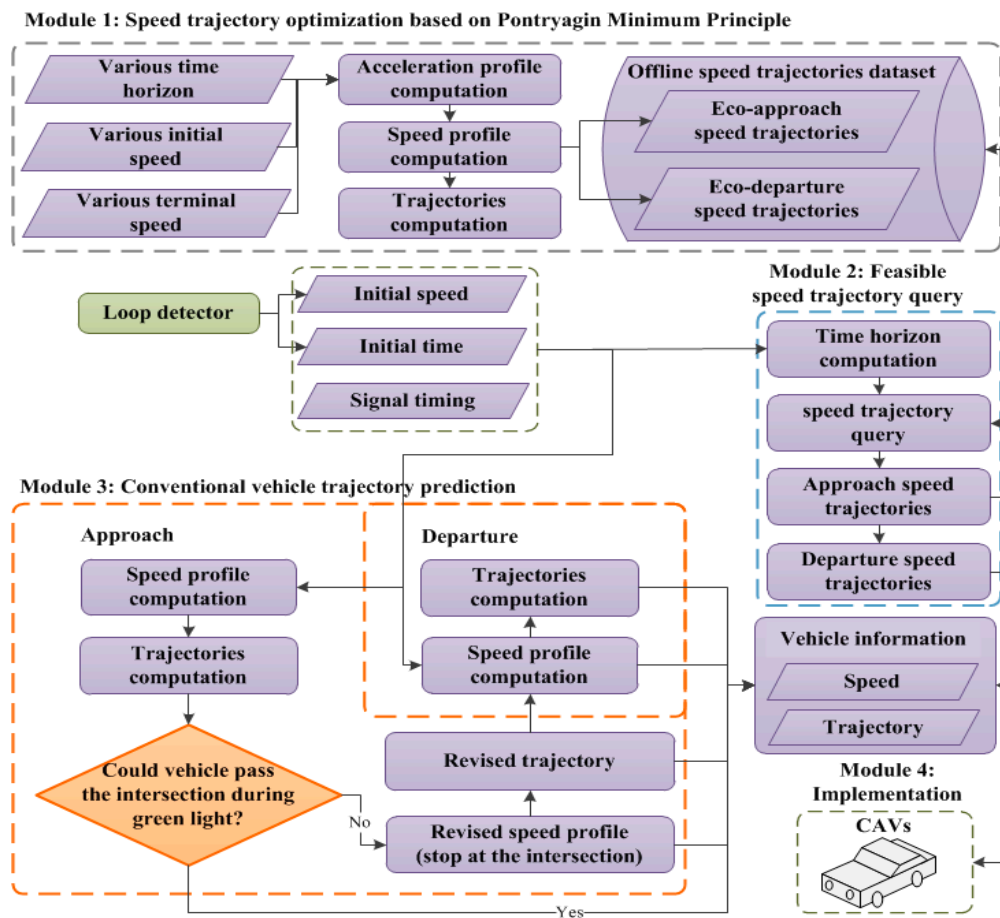


Figure 2. Control structure.

- Module 1:** Speed trajectory optimization based on Pontryagin Minimum Principle. In the control zone, the vehicle traveling is divided into three stages, including approach, turning and departure. Acceleration and deceleration maneuvers are only allowed in the approach and departure stages. All CAVs should maintain a constant longitudinal speed during left-turning, which means they travel at its terminal speed of approach stage in the intersection zone. Thus, the speed optimization focuses on the approach and departure stages. This module pre-generates various optimal eco-approach speed trajectories and eco-departure speed trajectories, and saving them in the database for module 2 to query and use. Each optimal speed trajectory has different combinations of time horizon, initial speed and terminal speed. Module 2 will query a feasible speed trajectory based on these attitudes.
- Module 2:** Feasible speed trajectory query. This module is activated when there is a CAV detected by the loop detector. The module first collects signal timing, CAV's current position and speed (position a in Figure 1), preceding vehicle's speed and spatial-temporal trajectories as inputs. Then it calculates the expected terminal time at the stop bar (position b in Figure 1) of approach stage which can force the CAV keep smallest headway with its preceding vehicle, and adopts maximum safe turning speed as terminal speed of approach stage to maximum the throughput at the intersection. Since the CAV will maintain maximum safe turning speed during traveling in the intersection zone, the initial time and speed of departure stage can be calculated. The initial time of departure stage (position c in Figure 1) is equal to the terminal time of approach stage plus the travel time in the intersection zone, and the initial speed of departure stage is equal to the maximum safe turning speed. Then this module calculates the expected terminal time at

the control zone boundary (position  $d$  in Figure 1) of departure stage with the consideration of preceding vehicle. The terminal speed of departure stage is set equal to the posted speed limit, so CAVs just need to cruise at high speed without any speed adjustment after exiting the control zone. Finally, this module sends a query request for feasible eco-approach and eco-departure speed trajectories to module 1. The query results are then transferred to CAV, and stored in vehicle information for future use.

- **Module 3: Conventional vehicle trajectory Prediction.** This module is activated when there is a conventional vehicle detected by the loop detector. Similar to module 2, this module also collect signal timing, conventional vehicle's current position and speed, preceding vehicle's speed and spatial-temporal trajectories as inputs, and then make a prediction of the conventional future speed and spatial-temporal trajectories by utilizing an improved Intelligent Driver Model (IDM) for signalized intersection proposed in previous study [35]. The predicted results are all stored in vehicle information for future use.
- **Module 4: Implementation.** The CAVs receive eco-approach and eco-departure speed trajectories from module 2 and adjust its speed accordingly.

### 3. Mathematical Formulations

This section presents the formulations of module 1, module 2 and module 3 in detail. Module 1 is entailed in Section 3.1, module 2 in Section 3.2 and module 3 in Section 3.3. The speed trajectory optimization is constructed in Pontryagin Minimum Principle (PMP) structure. The query terms of optimal speed trajectory include time horizon, initial and terminal speed. The motion of conventional vehicle is predicted by using an improved Intelligent Driver Model (IDM). The proposed prediction and optimization have the following assumptions:

- The desired speed of conventional vehicles equals to the posted speed limit on the road segment. These vehicles travel at posted speed limit unless impeded by its preceding vehicle.
- The CAVs adopt the optimized speed advisory as desired speed.
- Only longitudinal motion is focused in this study. No overtaking and weaving maneuvers are allowed in the control zone. These lateral motions would be considered in the next step improvement.

Detailed formulations of these three modules are presented in the following three sections. Table 1 lists the indices and parameters utilized hereafter.

**Table 1.** Indices and Parameters.

Notation	Meaning
$x_1(t)$	Vehicle position (m)
$x_2(t)$	Vehicle speed (m/s)
$u(t)$	Vehicle acceleration (m/s <sup>2</sup> )
$u_a(t)$	Predicted vehicle acceleration during approach stage in module 3 (m/s <sup>2</sup> )
$u_d(t)$	Predicted vehicle acceleration during departure stage in module 3 (m/s <sup>2</sup> )
$k(t)$	Vehicle jerk (m/s <sup>3</sup> )
$\Delta x_1(t)$	Distance gap of predicted vehicle to its preceding vehicle in module 3 (m)
$\Delta x_1^*(t)$	Desired gap of predicted vehicle to its preceding vehicle in module 3 (m)
$\Delta x_2(t)$	Speed difference of predicted vehicle to its preceding vehicle in module 3 (m/s)
$L$	Distance from initial position to terminal position (m)
$l$	Travel distance in the intersection zone (m)
$s_0$	Jam distance in module 3 (m)
$v_{lim}$	Posted speed limit of the road segment (m/s)
$v_{safe}$	Safe turning speed at the intersection (m/s)
$v_0$	Initial vehicle speed (m/s)
$v_a$	Vehicle speed at position a (m/s)
$v_f$	Preferred terminal speed (m/s)
$\underline{v}$	Minimum speed limit of CAV in module 1 (m/s)

Table 1. Cont.

Notation	Meaning
$\bar{u}$	Maximum vehicle acceleration (m/s <sup>2</sup> )
$\underline{u}$	Minimum vehicle acceleration (m/s <sup>2</sup> )
$u_{desired}$	Desired vehicle deceleration in module 3 (m/s <sup>2</sup> )
$\bar{k}$	Maximum vehicle jerk (m/s <sup>3</sup> )
$\underline{k}$	Minimum vehicle jerk (m/s <sup>3</sup> )
$T$	Safe time headway of two consecutive vehicles at the terminal position in module 3 (s)
$\delta$	Acceleration exponent
$t_0$	Initial time when vehicle reaches the initial position (s)
$t_f$	Terminal time when the CAV reaches the terminal position (s)
$t_a$	The arrival time of vehicle at the detector (location a), initial time of approach stage (s)
$t_b$	The arrival time of vehicle at the stop line (location b), terminal time of approach stage (s)
$t'_b$	The arrival time of preceding vehicle at the stop line (s)
$t_{b,early}$	Earliest arrival time of vehicle drives pass the stop line without considering its preceding vehicle and signal control (s)
$t_{b,candidate}$	Candidate arrival time of vehicle at the stop line (s)
$t_c$	The arrival time of vehicle at the boundary of intersection zone (location c), initial time of departure stage (s)
$t_d$	The arrival time of vehicle at the boundary of control zone (location d), terminal time of approach stage (s)
$t'_d$	The arrival time of preceding vehicle at the boundary of control zone (s)
$t_{d,early}$	Earliest time of CAV exit the control zone without considering its preceding vehicle (s)
$t_{horizon}$	Time horizon of approach or departure stage
$t_h$	Smallest headway of two consecutive vehicles at the stop line in module 2 (s)
$t_R$	The start time of red stage (s)
$t_{horizon}^{low-fuel}$	The time horizon of speed trajectory with lowest fuel consumption in the eco-departure speed trajectory dataset (s)
$g_t(t)$	Fuel consumption emissions rate of vehicle (mL/t)
$\alpha_j, \beta_1, \beta_2$	Parameters of fuel consumption and emissions model
$R$	Duration of red stage (s)
$G$	Duration of green stage (s)
$\zeta$	Collection of green stages
$\phi(x(t_f))$	Terminal cost of the optimal problem in module 1
$L(x(t), u(t))$	Running cost of the optimal problem in module 1
$C$	Constant value

### 3.1. Offline Speed Trajectories Optimization

#### 3.1.1. Speed Trajectory Optimization

##### 1. State Explanation

The state vector  $x(t)$  of a CAV is defined as follows.

$$x(t) = [x_1(t), x_2(t)]^T \quad (1)$$

The state dynamics is:

$$\dot{x}(t) = f(x(t), u(t)) = [x_2(t), u(t)]^T \quad (2)$$

The control input is the acceleration of CAV,  $u_n(t) = u_n(t)$ .

##### 2. Cost Function

The cost function is formulated as follows:

$$J = \phi(x(t_f)) + \int_0^{t_f} L(x(t), u(t)) dt \quad (3)$$

The controller enforces the terminal state to ensure the CAV can drive pass the terminal position on time at a preferred speed. The terminal cost is formulated as:

$$\phi(\mathbf{x}(t_f)) = w_1(x_1(t_f) - L)^2 + w_2(x_2(t_f) - v_f)^2, w_1 \in \mathbb{R}^+, w_2 \in \mathbb{R}^+ \quad (4)$$

where  $w_1$  and  $w_2$  are two large positive numbers which are used to ensure the constraint on CAV's final state.

The running cost is defined as follows:

$$L(\mathbf{x}(t), u(t)) = w_3 \cdot \frac{g_t(t)}{x_2(t)} + \frac{1}{2}u(t)^2, w_3 \in \mathbb{R}^+ \quad (5)$$

$$g_t(t) = \sum_{j=0}^3 \alpha_j \cdot x_2(t)^j + \beta_1 \cdot x_2(t) \cdot u(t) + \beta_2 \cdot x_2(t) \cdot u(t)^2 \cdot \chi(u(t)) \quad (6)$$

$$\chi(u(t)) = \begin{cases} 1 & u(t) \geq 0 \\ 0 & u(t) < 0 \end{cases} \quad (7)$$

where  $w_3$  is a weighting factor for fuel consumption and emissions, its unit is  $\text{m}^3/\text{mL} \cdot \text{s}^4$  [35].  $u(t)^2/2$  is the comfort consideration. The instantaneous fuel consumption rate  $g_t(t)$  is calculated by the fuel consumption and emissions model developed by Akcelik [41].

### 3. Conditions and Constraints

The initial conditions of vehicle are:

$$x_1(t_0) = 0, x_2(t_0) = v_0 \quad (8)$$

The cost function has following kinematic constraints, including speed, acceleration and jerk.

$$\nu_n = \{x_2 | \underline{v} \leq x_2(t) \leq v_{\text{lim}}, \forall t \in [0, t_f]\} \quad (9)$$

$$\mu = \{u | \underline{u} \leq u(t) \leq \bar{u}, \forall t \in [0, t_f]\} \quad (10)$$

$$k(t) = \frac{\partial u(t)}{\partial t} \quad (11)$$

$$\kappa = \left\{ k = \frac{\partial u(t)}{\partial t} \mid \underline{k} \leq k(t) \leq \bar{k}, \forall t \in [0, t_f] \right\} \quad (12)$$

### 4. Solution based on Pontryagin's Minimum Principle

The aforementioned speed trajectory optimization problem is solved using PMP approach. The Hamiltonian function is formulated as follows:

$$\begin{aligned} H(\mathbf{x}, \mathbf{u}, \boldsymbol{\lambda}, t) &= \boldsymbol{\lambda}^T \cdot \mathbf{f}(\mathbf{x}, \mathbf{u}, t) + L(\mathbf{x}, \mathbf{u}, t) \\ &= \lambda_1 \cdot x_2(t) + \lambda_2 \cdot u(t) + w_3 \left( \alpha_0 \cdot x_2(t)^{-1} + \alpha_1 + \alpha_2 \cdot x_2(t) + \dots \right. \\ &\quad \left. \alpha_3 \cdot x_2(t)^2 + \beta_1 \cdot u(t) + \beta_2 \cdot u(t)^2 \cdot \chi(u(t)) \right) + \frac{1}{2}u(t)^2 \end{aligned} \quad (13)$$

This necessary condition can be expressed alternatively as follows:

$$0 = \frac{\partial H}{\partial \mathbf{u}} \Rightarrow \begin{cases} u(t) = -\frac{\lambda_2 + w_3 \beta_1}{1 + 2w_3 \beta_2}, & \forall \lambda_2 \leq -w_3 \beta_1 \\ u(t) = -(\lambda_2 + w_3 \beta_1), & \forall \lambda_2 > -w_3 \beta_1 \end{cases} \quad (14)$$

$$\dot{\boldsymbol{\lambda}} = -\frac{\partial H}{\partial \mathbf{x}} \Rightarrow \begin{cases} \lambda_1 = C \\ \dot{\lambda}_2 = -\lambda_1 + w_3 \left( \alpha_0 \cdot x_2(t)^{-2} - \alpha_2 - 2\alpha_3 \cdot x_2(t) \right) \end{cases} \quad (15)$$

$$\dot{x} = \frac{\partial H}{\partial \lambda} \quad (16)$$

The Equations (14) and (15) are used to solve the optimal control  $u^*$  and Equation (16) is same as state dynamics.

As stated before, the desired terminal state  $\phi(x(t_L))$  should be enforced to ensure the CAV can drive pass the terminal position on time at a preferred speed. The co-state  $\lambda$  should satisfy the following condition:

$$\lambda(t_f) = \frac{\partial \phi(x(t_f))}{\partial x} \Rightarrow \begin{cases} \lambda_1(t_f) = 2w_1(x_1(t_f) - L) \\ \lambda_2(t_f) = 2w_2(x_2(t_f) - v_f) \end{cases} \quad (17)$$

Then a numerical solution is adopted to solve the aforementioned problem. The main idea is to iteratively find state  $x$  forward in time and then co-state  $\lambda$  backward in time. Interested readers could refer to these papers [9,18,35] for the detailed algorithm.

### 3.1.2. Eco-Approach and Departure Speed Trajectory Dataset

The offline speed trajectories dataset stores amounts of optimal speed trajectories that are generated by using the aforementioned speed trajectory optimization. As shown in Figure 2, all these optimal speed trajectories should be generated before the system is implemented. There are two sub-datasets in the offline dataset, including eco-approach speed trajectory dataset and eco-departure speed trajectory dataset.

#### 1. Eco-approach speed trajectories dataset

In this system, all optimization should be completed before the implementation of system. For simplicity, the initial time of all eco-approach speed trajectories is set to zero. The initial conditions for eco-approach speed trajectories are defined as follows:

$$t_0 = 0 \quad (18)$$

$$x_1(t_0) = 0, x_2(t_0) = v_0 \quad (19)$$

As stated in Section 2, the controller enforces the terminal state of approach stage to maximize the throughput at the intersection. All the CAVs are forced to pass through the intersection at maximum safe left-turning speed,  $v_f = v_{safe}$ . The terminal state is:

$$t_f = t_0 + t_{horizon} = t_{horizon} \quad (20)$$

$$x(t_f) = (L, v_{safe})^T \quad (21)$$

As shown in above four equations,  $t_0$ ,  $x_1(t_0)$ ,  $x_1(t_f)$  and  $x_2(t_f)$  are constant for all speed trajectories, only  $x_2(t_0)$  and  $t_f$  are variable and different for each speed trajectory. To reduce the size of dataset, only integral values are taken for the initial speed and optimization time horizon. Thus the eco-approach speed trajectory dataset is defined as follows:

$$V_{approach} = \left\{ V_{approach}^{v_0, t_{horizon}} \mid v_0 \in \mathbf{N}_+ \cap (0, v_{lim}), t_{horizon} \in \mathbf{N}_+ \cap \left( \frac{L}{v_{lim}}, \frac{L}{\underline{v}} \right) \right\} \quad (22)$$

Each speed trajectory in the dataset has two attributes of initial speed and optimization time horizon. The controller would query the dataset for a feasible eco-approach speed trajectory by these two attributes.

## 2. Eco-departure speed trajectories dataset

The initial time of eco-departure speed trajectory is also set to zero. Since the CAVs are assumed to maintain maximum safe turning speed during traveling in the intersection zone, the initial speed of eco-departure speed trajectory is equal to the maximum safe turning speed. The initial conditions are defined as follows:

$$t_0 = 0 \quad (23)$$

$$x_1(t_0) = 0, x_2(t_0) = v_{safe} \quad (24)$$

As stated in Section 2, all CAVs would be forced to accelerate to the posted speed limit before exiting the control zone,  $v_f = v_{lim}$ . Then CAVs just need to ecologically cruise at high speed on the road. The terminal state is:

$$t_f = t_0 + t_{horizon} = t_{horizon} \quad (25)$$

$$\mathbf{x}(t_f) = (L, v_{lim})^T \quad (26)$$

As shown in above three equations,  $t_0$ ,  $x_1(t_0)$ ,  $x_1(t_f)$ ,  $x_2(t_0)$  and  $x_2(t_f)$  are constant for all speed trajectories, only  $t_f$  are variable and different for each speed trajectory. Only integral values are taken for the optimization time horizon. Thus the eco-departure speed trajectory dataset is defined as follows:

$$V_{departure} = \left\{ V_{departure}^{t_{horizon}} \mid t_{horizon} \in \mathbf{N}_+ \cap \left( \frac{L}{v_{lim}}, \frac{L}{\underline{v}} \right) \right\} \quad (27)$$

Each speed trajectory in the dataset has only one attribute of optimization time horizon. The controller would query the dataset for a feasible eco-departure speed trajectory by this attribute.

### 3.2. Feasible Speed Trajectory Query

This module is activated when a CAV drive pass the loop detector, and collects signal timing, CAV's current position and speed, preceding vehicle's speed and spatial-temporal trajectories as input. Then it calculates expected terminal time of approach and departure stages.

As stated in Section 2, the controller forces CAV keep smallest headway with its preceding vehicle at the intersection to maximize the throughput. The expected terminal time of approach stage should be calculated as follows:

$$t_{b,candidate} = \max(t'_b + t_h, t_{b,early}) \quad (28)$$

$$t_{b,early} = t_a + \frac{L - \left( \frac{v_{lim}^2 - x_2(t_a)^2}{2\underline{u}} \right) - \left( \frac{v_{lim}^2 - v_{safe}^2}{2\underline{u}} \right)}{v_{lim}} + \frac{v_{lim} - x_2(t_a)}{\underline{u}} + \frac{v_{lim} - v_{safe}}{\underline{u}} \quad (29)$$

$$t_b = \begin{cases} t_{b,candidate}, & \forall t_{b,candidate} \in \zeta \\ \left\lfloor \frac{t_{b,candidate}}{R+G} \right\rfloor \cdot (R+G) + R, & \forall t_{b,candidate} \notin \zeta \end{cases} \quad (30)$$

The feasible eco-approach speed trajectory is  $V_{approach}^{v_0=v_a, t_{horizon}=\lceil t_b-t_a \rceil}$ .

During departure stage, the controller forces CAV accelerate to legal speed limit before exiting the control zone, the expected terminal time of departure stage should be calculated as follows:

$$t_c = t_b + \frac{l}{v_{safe}} \quad (31)$$

$$t_d = \max(t'_d + t_h, t_{d,early}) \quad (32)$$

$$t_{d,early} = t_c + \frac{v_{lim} - v_{safe}}{\underline{u}} + \frac{L - \left( \frac{v_{lim}^2 - v_{safe}^2}{2\underline{u}} \right)}{v_{lim}} \quad (33)$$

The feasible eco-departure speed trajectory is:  $V_{departure}^{t_{horizon}=\max(\lceil t_d-t_c \rceil, t_{horizon}^{low-fuel})}$ . It means that the CAV would choose an earliest eco-departure speed trajectory when it is impeded by preceding vehicle, and choose a most ecological speed trajectory without impediment of surrounding traffic.

### 3.3. Conventional Vehicle Trajectory Prediction

The longitudinal dynamics model of conventional vehicle comes from the Intelligent Driver Model (IDM). During approach stage, signal control can over-rule the car-following model. The acceleration trajectory of approach stage can be formulated as follows:

$$u_a(t) = \bar{u} \left[ 1 - \left( \frac{x_2(t)}{v_{lim}} \right)^\delta - \left( \frac{\Delta x_1^*(x_2(t), \Delta x_2(t))}{\Delta x_1(t)} \right)^2 \right], \forall t_b \in \zeta, t \in [t_a, t_b] \quad (34)$$

$$u_a(t) = \begin{cases} \bar{u} \left[ 1 - \left( \frac{x_2(t)}{v_{lim}} \right)^\delta - \left( \frac{\Delta x_1^*(x_2(t), \Delta x_2(t))}{\Delta x_1(t)} \right)^2 \right], \forall t_b \notin \zeta, t \notin [t_a, t_b] \cap [t_R, t_R + R] \\ \bar{u} \left[ 1 - \left( \frac{x_2(t)}{v_{lim}} \right)^\delta - \left( \frac{\Delta x_1^*(x_2(t), x_2(t))}{L - x_1(t)} \right)^2 \right], \forall t_b \notin \zeta, t \in [t_a, t_b] \cap [t_R, t_R + R] \end{cases} \quad (35)$$

$$t_R = \left\lfloor \frac{t_b}{R + G} \right\rfloor \cdot (R + G), \forall t_b \notin \zeta \quad (36)$$

$$\Delta x_1^*(x_2(t), \Delta x_2(t)) = s_0 + \max \left( x_2(t) \cdot T + \frac{x_2(t) \cdot \Delta x_2(t)}{2\sqrt{\bar{u}} \cdot u_{desired}}, 0 \right) \quad (37)$$

$$\Delta x_1^*(x_2(t), x_2(t)) = s_0 + \max \left( x_2(t) \cdot T + \frac{x_2(t)^2}{2\sqrt{\bar{u}} \cdot u_{desired}}, 0 \right) \quad (38)$$

The Equation (34) shows that the conventional vehicle and its preceding vehicle can enter the intersection in the same green phase. The Equation (35) shows that the conventional vehicle and its preceding vehicle cannot enter the intersection in the same green phase.

During departure stage and traveling in the intersection zone, only the preceding vehicle has some impacts on conventional vehicle. The acceleration trajectory of departure stage can be calculated by using original IDM model as follows:

$$u_d(t) = \bar{u} \left[ 1 - \left( \frac{x_2(t)}{v_{lim}} \right)^\delta - \left( \frac{\Delta x_1^*(x_2(t), \Delta x_2(t))}{\Delta x_1(t)} \right)^2 \right], \forall t \in [t_b, \infty) \quad (39)$$

$$\Delta x_1^*(x_2(t), \Delta x_2(t)) = s_0 + \max \left( x_2(t) \cdot T + \frac{x_2(t) \cdot \Delta x_2(t)}{2\sqrt{\bar{u}} \cdot u_{desired}}, 0 \right) \quad (40)$$

## 4. Simulation and Evaluation

### 4.1. Simulation Platform and Setup

This eco-approach and departure system is evaluated through a microscope simulation, and applied to a hypothetical signalized intersection. As shown in Figure 1, only Northbound (NB) and Southbound (SB) are with exclusive left-turn lanes. Due to that the proposed system only focuses on the longitudinal motion of vehicles, no weaving and overtaking maneuvers are allowed in the control zone. To avoid conflicts between left-turn traffic flow and straight-going traffic flow, the signal timing plan provides exclusive left-turn phase for the left-turn traffic on these two directions. Loop detectors are installed on the left-turn lanes at the boundary of control zone. This test network has been calibrated according to the Highway Capacity Manual 2010, the saturated traffic flow on each left-turn lane is equal to 1780 veh/h. Since the left-turn traffic from both directions have the same traffic

conditions, only the traffic on NB approach is evaluated in this study. The setups of the simulation are shown in Table 2. The distance of approach and departure is calculated as follows.

$$L = \underline{v} \cdot n \cdot (R + G) \quad (41)$$

where  $\underline{v}$  represents the minimum speed limit of connected and automated vehicles,  $R$  and  $G$  are the duration of red phase and the duration of green phase,  $n$  is a positive value. As the results in previous studies, some vehicles spent time more than one cycle of traffic signal to travel from the loop detector to the stop bar [35]. To ensure each CAV could obtain an available optimal speed trajectory from the offline speed trajectory dataset, the parameter  $n$  should be not less than 2. Thus, the approach or departure distance  $L$  is set to the nearest hundreds to simplify the setup, as shown in Table 2.

**Table 2.** Setups of the simulation.

Parameter	Value
<i>VISSIM</i>	
Approach or departure distance $L$ (m)	300
Travel distance in the intersection zone $l$ (m)	20
Duration of simulation (s)	1200
Signal control cycle (s)	60
Duration of red light $R$ (s)	42
Duration of green light $G$ (s)	18
<i>Module 1 and Module 2</i>	
Posted speed limit $v_{lim}$ (m/s)	20 ( $\approx 45$ mph)
Minimum speed limit $\underline{v}$ (m/s)	2.2 ( $\approx 5$ mph)
Safe turning speed $v_{safe}$ (m/s)	11 ( $\approx 25$ mph)
Maximum acceleration $\bar{u}$ (m/s <sup>2</sup> )	3.5
Minimum acceleration $\underline{u}$ (m/s <sup>2</sup> )	−4
Maximum jerk $\bar{k}$ (m/s <sup>3</sup> )	10
Minimum jerk $\underline{k}$ (m/s <sup>3</sup> )	0
Pre-set headway $t_h$ (s)	2.3
Weighting factors ( $w_1, w_2, w_3$ )	(10,100,1)
<i>Module 3</i>	
Minimum speed (m/s)	0
Safe time headway $T$ (s)	1.8
Desired deceleration $u_{desired}$ (m/s <sup>2</sup> )	−2.8
Acceleration exponent $\delta$	4
Jam distance $s_0$ (m)	5

The simulation runs on an integrated simulation platform proposed in previous eco-driving study [35]. To truly simulate the real traffic where the CAV may be impeded by its preceding vehicle and cannot drive at the advisory speed, the eco-approach and departure speed trajectories are sent to the CAVs as “Desired speed”. The actual speed of CAVs may be inconsistent with the optimized speed.

The eco-approach and departure system is evaluated on two traffic-related factors, including congestion level (CL) and market penetration rate (MPR) of CAVs. The measures of effectiveness (MOEs) are terminal speed of eco-approach, throughput, fuel consumption and CO<sub>2</sub> emission. To fairly confirm the ecological benefits of the system, the fuel consumption and CO<sub>2</sub> emission are calculated by VT-Micro fuel consumption and emission model instead of the model in Equation (6). The baseline scenario is set as 0% MPR of CAVs, which means no CAV can be controlled. The eco-approach and departure scenario is set as when partly or all vehicles are CAVs. All the vehicles have the same size and kinematics characteristics. The vehicle arrival pattern obeys the Poisson distribution. The computation and query time for each individual CAV is collected to evaluate the timeliness of the system. The formulations of benefits are defined as follows:

$$B_{throughput} = \frac{TP_e - TP_b}{TP_b} \times 100\% \quad (42)$$

$$B_{fuel-efficiency} = \frac{FE_e - FE_b}{FE_b} \times 100\% \quad (43)$$

$$B_{CO_2-emission} = \frac{CE_b - CE_e}{CE_b} \times 100\% \quad (44)$$

where  $B_{throughput}$ ,  $B_{fuel-efficiency}$  and  $B_{CO_2-emission}$  represent the throughput, fuel consumption and CO<sub>2</sub> emission benefits respectively;  $TP_b$ ,  $FE_b$  and  $CE_b$  are throughput, fuel efficiency and CO<sub>2</sub> emission in the baseline scenario;  $TP_e$ ,  $FE_e$  and  $CE_e$  are throughput, fuel efficiency and CO<sub>2</sub> emission in the eco-approach and departure control scenario.

#### 4.2. Simulation Results

The simulation and evaluation results are illustrated in this section. The eco-approach and departure system achieve the expected objectives: forces all CAVs adjust their speed to maximum safe turning speed before entering the intersection, maintains optimal mobility status for the intersection while improving fuel efficiency and emission reduction during the whole approach and departure stage.

Figure 3 shows the frequency distribution of computation and query time in module 2. The computation and query time is at a  $10^{-5}$  s level, it is much lower than the computation time of online optimization in previous study which is at a  $10^{-1}$  s level [35]. The proposed eco-approach and departure system significantly reduce the computation time to lower than the update interval of real-time speed control on the future CAVs with high control frequency ( $10^{-1}$  s) [8,35]. It has clear relevance and can be used for real-time applications in the near future.

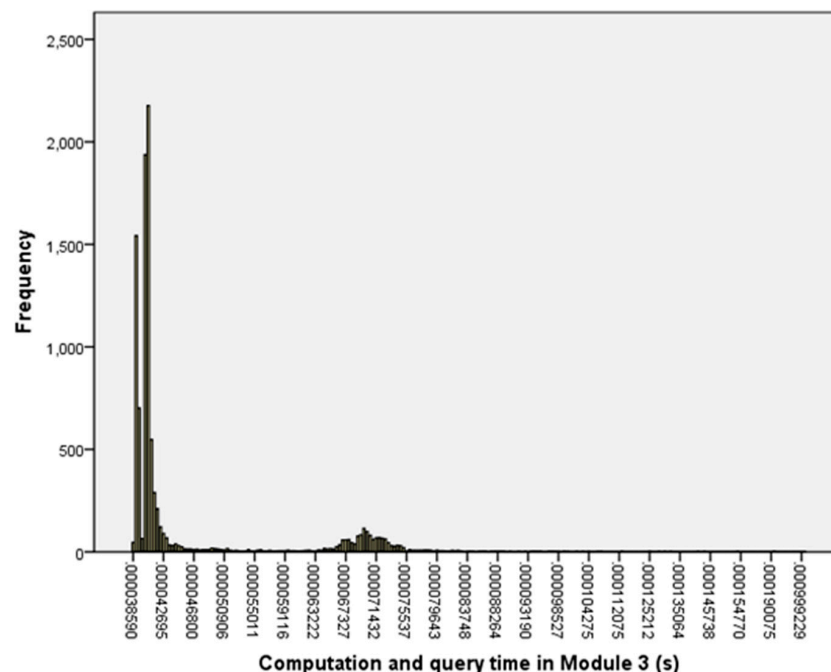


Figure 3. Computation and query time in Module 2.

The vehicle which can drive pass the stop bar at a safe turning speed is named as “safe vehicle” in this study. Figure 4 shows the increase in percentage of safe vehicles under various levels of CL and MPR of CAVs. Significant increase in percentage of safe vehicles can be observed under

various CL levels when the MPR of CAVs is greater than or equal to 10%. Under non-saturated and saturated conditions, higher increase in percentage of safe vehicles was achieved with higher MPR of CAVs. The increase in percentage of safe vehicles under non-saturated condition is higher than under saturated condition at the same level of MPR of CAVs. Fewer vehicles drove pass the intersection at a speed higher than maximum turning speed when the proposed system was implemented. In other words, the proposed system can effectively increase the proportion of safe vehicles so as to enhance the traffic safety at the intersection.

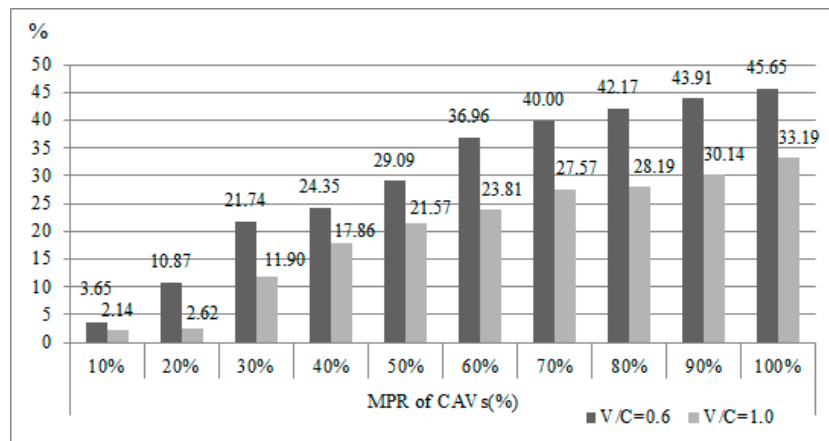


Figure 4. Increase in percentage of safe vehicles.

Figure 5 shows the throughput benefits under various levels of CL and MPR of CAVs. No significant throughput benefits can be observed under different conditions. The proposed system has no adverse effect on the mobility. In other words, the proposed system could maintain optimal mobility under different traffic conditions, unlike some previous eco-driving system that has negative impacts on throughput at the intersection under high congestion levels [16,22,38,39].

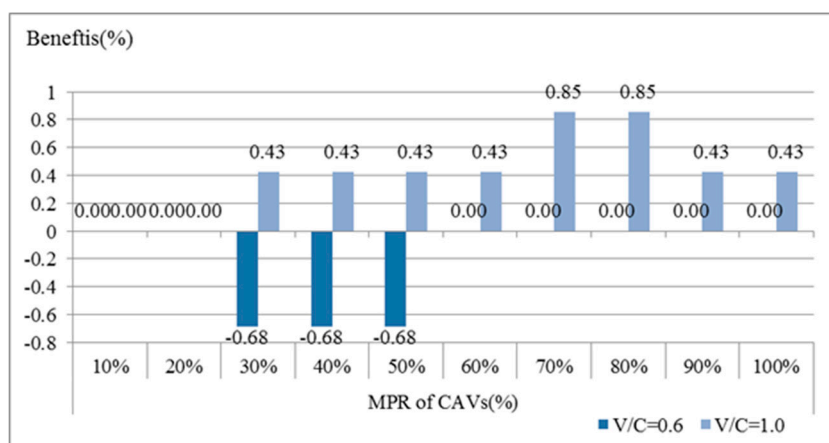


Figure 5. Improvements of throughput.

Figure 6 shows the fuel consumption benefits under various levels of CL and MPR of CAVs. The proposed system generates significant benefits on fuel efficiency as long as CAV is introduced. The benefits show a growing trend as the MPR of CAVs increases under these two different congestion levels. This growing trend levels off at 50% MPR of CAVs. Moreover, the benefit under saturated condition is higher than under non-saturated condition at the same MPR level. The proposed system can effectively improve the fuel efficiency.

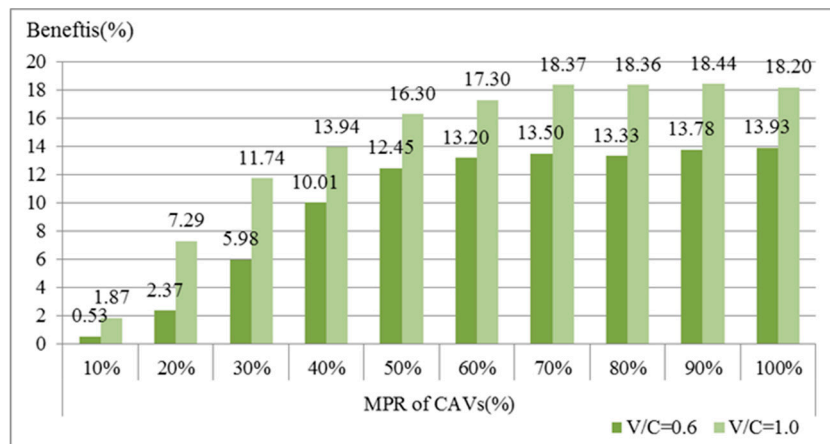


Figure 6. Improvements of fuel efficiency.

Figure 7 shows the CO<sub>2</sub> emission benefits under various levels of CL and MPR of CAVs. Significant benefits can be observed under different conditions. The benefits grow with the congestion level and MPR of CAVs. The proposed system can effectively reduce the CO<sub>2</sub> emission.

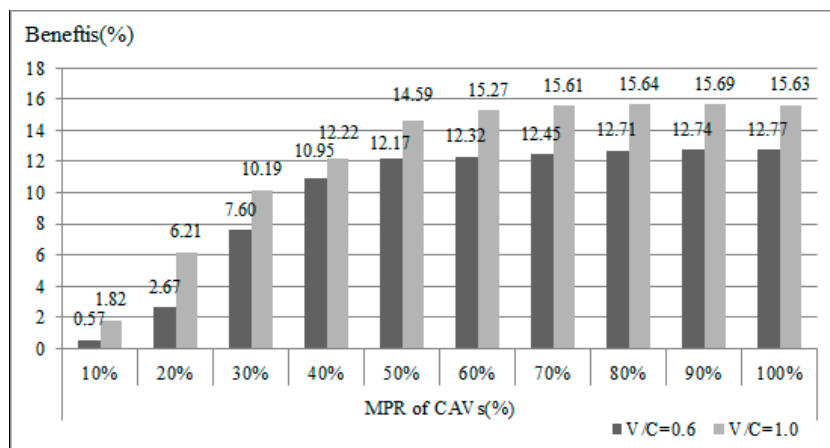


Figure 7. Improvements of CO<sub>2</sub> emission.

All the above results show that the proposed system is able to improve the fuel efficiency and CO<sub>2</sub> emission reduction while maintaining optimal mobility status at the intersection when the MPR of CAVs is greater than or equal to 10%. This phenomenon indicates that the proposed system could be beneficial under low level of MPR of CAVs, similar to the eco-approach control system proposed in the previous study that is also able to function when the MPR of CAVs is not less than 10% [35]. The proposed system can be applied in the real traffic as long as CAV is legalized and introduced in the near future.

Figure 8 shows the spatial-temporal trajectories of simulation results under non-saturated and saturated conditions. Figure 8a,b show the spatial-temporal trajectories in baseline scenarios. Figure 8c–l show the spatial-temporal trajectories in eco-approach and departure scenarios. The comparison between the baseline trajectories and eco-driving trajectories confirms that the CAVs could smoothly approach and depart the intersection, and have significant impacts on the following conventional human-driven vehicles. The smooth spatial-temporal trajectories effectively improve the vehicles’ fuel efficiency and reduce their emissions. As the MPR of CAVs increases, fewer vehicles need to stop and idle at the intersection to wait for green light, and fewer conventional vehicles choose to sharply accelerate to their desired speed after driving pass the intersection. Most vehicles have an

ecological trajectory when the MPR of CAVs is greater than 40%. This can explain why the increasing trend of fuel consumption benefits levels off at 50% MPR of CAVs.

Besides, the CAV's deceleration during approaching the intersection forces vehicles into tight marching platoons. At the same level of MPR of CAVs, the platoons under saturated condition are much tighter than under non-saturated condition. A smaller headway can be observed under heavy traffic. The following conventional vehicles have more similar spatial-temporal trajectories to their preceding CAV. In other words, the CAVs have greater impacts on their following conventional vehicles under higher congestion level. This is consistent with the findings from the improvements of fuel consumption and CO<sub>2</sub> emissions.

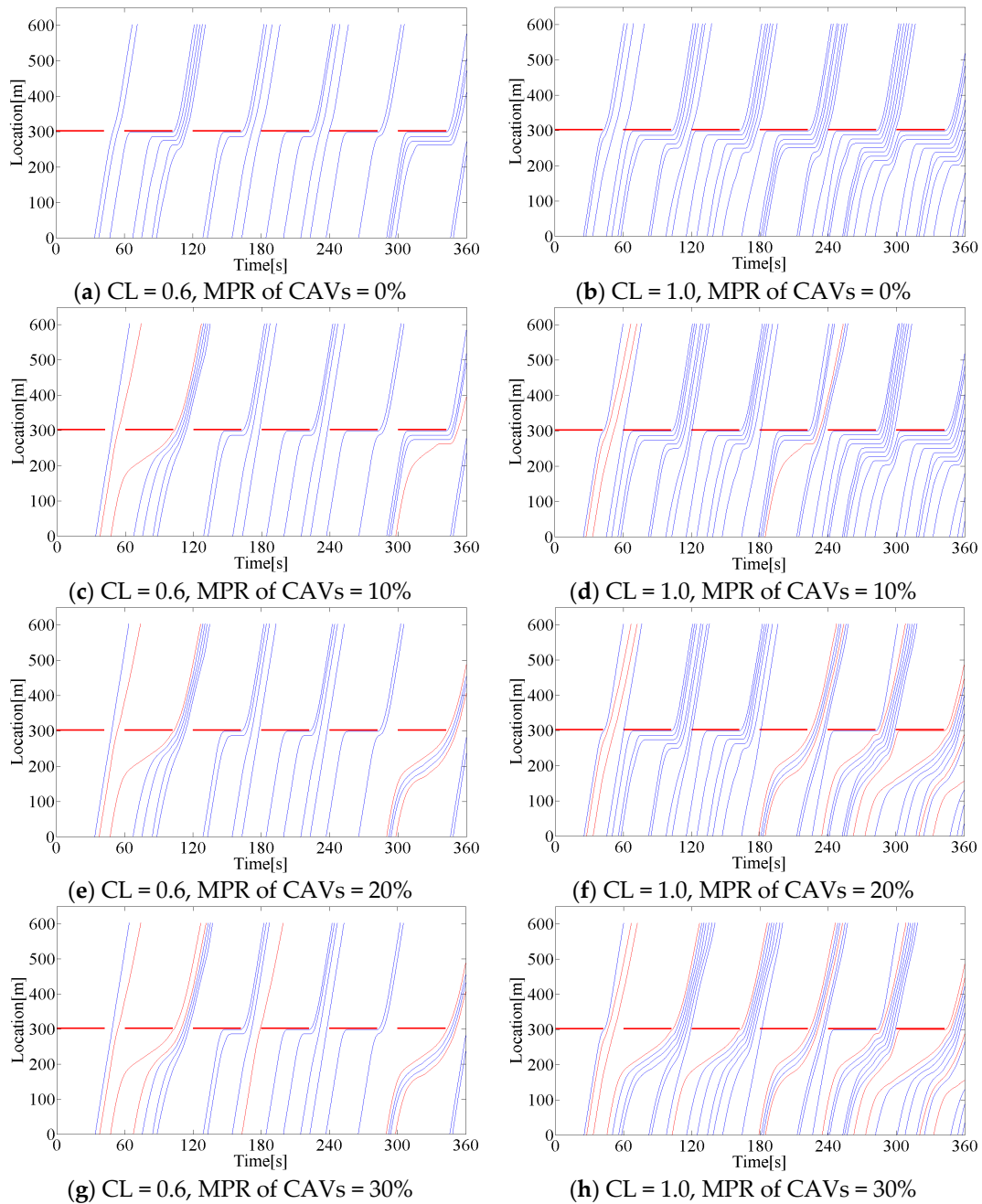


Figure 8. Cont.

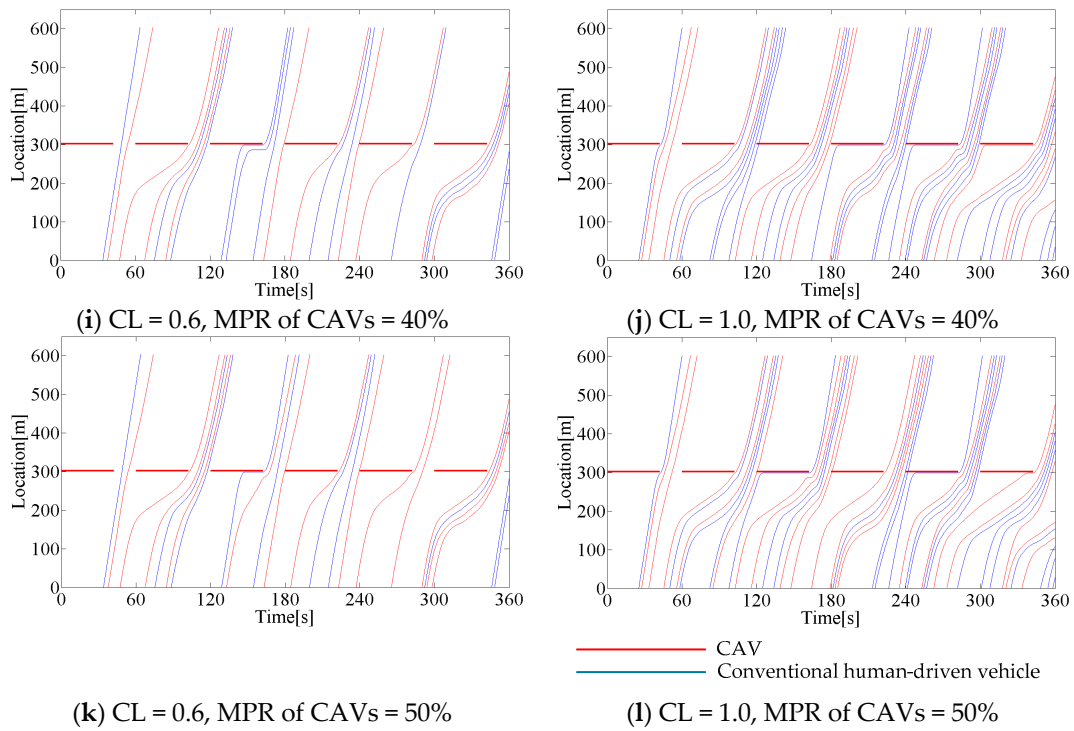


Figure 8. Spatial-temporal trajectories of simulation results.

Figure 9 shows the sample speed trajectories of CAVs under different congestion levels. The red curves are speed trajectories generated by eco-approach and departure controller and named as “Calculated speed trajectory”, the blue curves are “Real” speed trajectories collected in the simulation and named as “simulated speed trajectory”. There exist some deviations between the calculated and simulated speed trajectories due to that the optimized speed trajectories are adopted by CAVs as desired speed. The CAVs may exceed the advisory speed when they are far away from its preceding vehicle, and much lower than the advisory speed when they are impeded by its preceding conventional vehicle. The deviations indicate that the proposed system is robust to the randomness of traffic.

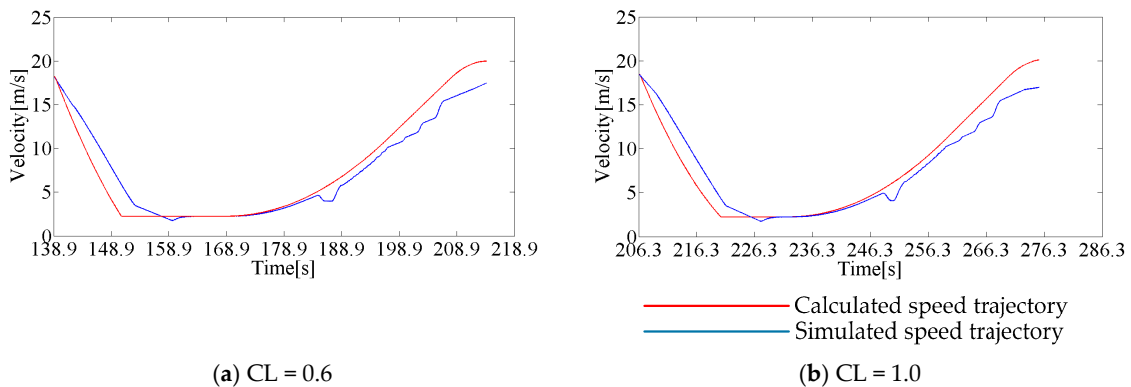


Figure 9. Speed trajectories of optimization and simulation results.

5. Conclusions and Future Research

This research proposed an eco-approach and departure system for left-turn vehicles at signalized intersection under partially connected and automated vehicles environment. The proposed system is improved from an existing eco-approach control system for straight-going vehicles. It can significantly

enhance the traffic safety for left-turn vehicles while improving the fuel efficiency and emission reduction without any adverse effect on mobility. Its major advantages includes: (i) greatly reducing the computation time which makes the proposed eco-approach and departure system more feasible for implementation in real traffic networks; (ii) significantly enhancing the traffic safety at the intersection; (iii) improving the fuel efficiency and emission reduction within the control zone by providing both eco-approach and eco-departure speed trajectories for each CAV. The core module of proposed system, offline speed trajectories optimization was formulated based on Pontryagin's Minimum Principle structure. The detailed evaluation showed:

- The computation time for speed trajectory query in module 2 ranges from  $3.86 \times 10^{-5}$  to  $9.99 \times 10^{-3}$ . The proposed eco-approach and departure system is a truly real-time control system compared to the previous eco-driving system.
- The percentage of safe vehicles increases by 3.65% to 45.65% under non-saturated condition, and increases by 2.14% to 33.19% under saturated condition. The percentage grows with the market penetration rate of CAVs and congestion level. The proposed eco-approach and departure system significantly enhance the traffic safety at the intersection by reducing the over-speed vehicles.
- Throughput benefits range from  $-0.68\%$  to  $0\%$  under non-saturated condition, and range from  $0\%$  to  $0.85\%$  under saturated condition. Such little benefits have no significant impact on the throughput. The proposed eco-approach and departure system maintains the mobility at its optimal level.
- Fuel consumption benefits range from  $0.53\%$  to  $13.93\%$  under non-saturated condition, and range from  $1.87\%$  to  $18.44\%$  under saturated condition. CO<sub>2</sub> emission benefits range from  $0.57\%$  to  $12.77\%$  under non-saturated condition, and range from  $1.82\%$  to  $15.69\%$  under saturated condition. All these two kinds of benefits increase with the market penetration rate of CAVs and congestion level.
- Similar to the previous eco-approach system for straight-going vehicles, the proposed eco-approach and departure system is also able to be beneficial under low market penetration rate of CAVs, which means it can be implemented in the real traffic as long as CAV is introduced in the near future.
- The proposed eco-approach and departure system has a good robustness against the randomness of traffic.

Future research should focus on designing a lateral control strategy for vehicles' lateral motions, and improve the longitudinal control method to prevent or reduce the disturbance caused by lateral motions. Then the improved eco-approach and departure system can be applied in multi-lanes network with overtaking and weaving maneuvers. Furthermore, a field evaluation on the proposed eco-approach and departure system should be designed and conducted to analyze the benefits of system implemented in the real traffic, and find out the improvement room for future research.

**Acknowledgments:** This research was in part supported by the Chinese National Natural Science Funds No.71390522 and No.51578199 funded by the National Natural Science Foundation of China (NSFC).

**Author Contributions:** Huifu Jiang and Shi An conceived and designed the proposed system; Jianxun Cui designed and performed the simulation; Huifu Jiang analyzed the simulation results; Huifu Jiang and Jian Wang wrote the paper.

**Conflicts of Interest:** The authors declare no conflict of interest. The founding sponsors had no role in the design of the study; in the collection, analyses, or interpretation of data; in the writing of the manuscript, and in the decision to publish the results.

## References

1. U.S. Environmental Protection Agency. Sources of Greenhouse Gas Emission. Available online: <https://www3.epa.gov/climatechange/ghgemissions/sources/transportation.html> (accessed on 25 April 2016).
2. FHWA. Connected Vehicle Eco GlidePath at Signalized Intersections. Available online: <http://higherlogicdownload.s3.amazonaws.com/AUVSI/c2a3ac12-b178-4f9c-a654-78576a33e081/UploadedImages/Proceedings/Posters/USDOT/DOT%202012%20Connected%20Vehicle%20Eco%20GlidePath%20at%20Signalized%20Intersections.pdf> (accessed on 1 November 2016).

3. Hoed, R.V.D.; Harmelink, M.; Joosen, S. Evaluation of the Dutch Eco-Driving Programme. EIE-2003-114 AID-EE Project: Project Executed within the Frame-Work of Energy Intelligence for Europe Program. 2006. Available online: <https://www.ecofys.com/files/files/aid-ee-2006-evaluation-ecodrive-netherlands.pdf> (accessed on 1 November 2016).
4. IEA. Energy Policies of IEA Countries: Japan (International Energy Agency). Available online: <http://www.iea.org/textbase/nppdf/free/2008/japan2008.pdf> (accessed on 18 August 2012).
5. National Transportation Library. Available online: [http://ntl.bts.gov/lib/44000/44600/44661/FHWA-JPO-11-139\\_AERIS\\_Applications\\_SOP\\_Report-FINAL\\_081211-REV\\_9-13-11.pdf](http://ntl.bts.gov/lib/44000/44600/44661/FHWA-JPO-11-139_AERIS_Applications_SOP_Report-FINAL_081211-REV_9-13-11.pdf) (accessed on 2 January 2014).
6. Wada, T.; Yoshimura, K.; Doi, S.I. Proposal of an eco-driving assist system adaptive to driver's skill. In Proceedings of the International IEEE Conference on Intelligent Transportation Systems, Washington, DC, USA, 5–7 October 2011; pp. 1880–1885.
7. Durbin, T.D.; Miller, J.W.; Johnson, K.; Hajbabaie, M.; Kado, N.Y.; Kobayashi, R.; Liu, X.; Vogel, C.F.; Matsumura, F.; Wong, P.S. *Biodiesel Characterization and NOx Mitigation Study*; Final Report; CARB Assessment of the Emissions from the Use of Biodiesel as a Motor Vehicle Fuel in California; California Air Resources Board: Sacramento, CA, USA, 2011.
8. Hu, J.; Shao, Y.; Sun, Z.; Wang, M.; Bared, J.; Huang, P. Integrated optimal eco-driving on rolling terrain for hybrid electric vehicle with vehicle-infrastructure communication. *Transp. Res. Part C* **2016**, *68*, 228–244. [[CrossRef](#)]
9. Zegeye, S.K.; De Schutter, B.; Hellendoorn, J.; Breunese, E.A. Variable speed limits for green mobility. In Proceedings of the 2011 14th International IEEE Conference on Intelligent Transportation Systems (ITSC), Washington, DC, USA, 5–7 October 2011; pp. 2174–2179.
10. Ghassan, A. Integrated Adaptive-Signal Dynamic-Speed Control of Signalized Arterials. *J. Transp. Eng.* **2002**, *128*, 447–451.
11. Barth, M.; Boriboonsomsin, K. Energy and emissions impacts of a freeway-based dynamic eco-driving system. *Transp. Res. Part D* **2009**, *14*, 400–410. [[CrossRef](#)]
12. Wang, M.; Daamen, W.; Hoogendoorn, S.P.; van Arem, B. Rolling horizon control framework for driver assistance systems. Part I: Mathematical formulation and non-cooperative systems. *Transp. Res. Part C* **2014**, *40*, 271–289. [[CrossRef](#)]
13. Wang, M.; Daamen, W.; Hoogendoorn, S.P.; van Arem, B. Rolling horizon control framework for driver assistance systems. Part II: Cooperative sensing and cooperative control. *Transp. Res. Part C* **2014**, *40*, 290–311. [[CrossRef](#)]
14. Chen, Y.; Zhang, D.; Li, K. Enhanced eco-driving system based on V2X communication. In Proceedings of the International IEEE Conference on Intelligent Transportation Systems, Anchorage, AK, USA, 16–19 September 2012; pp. 200–205.
15. Mandava, S.; Boriboonsomsin, K.; Barth, M. Arterial velocity planning based on traffic signal information under light traffic conditions. In Proceedings of the 2009 12th International IEEE Conference on Intelligent Transportation Systems, St. Louis, MO, USA, 4–7 October 2009; pp. 1–6.
16. Barth, M.; Mandava, S.; Boriboonsomsin, K.; Xia, H. Dynamic ECO-driving for arterial corridors. In Proceedings of the 2011 IEEE Forum on Integrated and Sustainable Transportation System (FISTS), Vienna, Austria, 29 June–1 July 2011; pp. 182–188.
17. Lee, J.; Park, B. Development and evaluation of a cooperative vehicle intersection control algorithm under the connected vehicles. *IEEE Trans. Intell. Transp. Syst.* **2012**, *13*, 81–90. [[CrossRef](#)]
18. Ma, J.; Li, X.; Zhou, F.; Hu, J.; Park, B. Parsimonious shooting heuristic for trajectory design of connected automated traffic part II: Computational issues and optimization. *Transp. Res. Part B* **2017**, *95*, 421–441. [[CrossRef](#)]
19. Zhou, F.; Li, X.; Ma, J. Parsimonious shooting heuristic for trajectory design of connected automated traffic part I: Theoretical analysis with generalized time geography. *Transp. Res. Part B* **2017**, *95*, 394–420. [[CrossRef](#)]
20. Ben, D. Fuel estimation model for ECO-driving and ECO-routing. *Intell. Veh. Symp.* **2011**, *30*, 37–42. [[CrossRef](#)]
21. Saboohi, Y.; Farzaneh, H. Model for developing an eco-driving strategy of a passenger vehicle based on the least fuel consumption. *Appl. Energy* **2009**, *86*, 1925–1932. [[CrossRef](#)]
22. Xia, H.; Boriboonsomsin, K.; Schweizer, F.; Winckler, A.; Zhou, K.; Zhang, W.B.; Barth, M. Field operational testing of eco-approach technology at a fixed-time signalized intersection. In Proceedings of the 2012 15th

- International IEEE Conference on Intelligent Transportation Systems (ITSC), Anchorage, AK, USA, 16–19 September 2012; pp. 188–193. [[CrossRef](#)]
23. Li, M.; Boriboonsomsin, K.; Wu, G.; Wei, Z.; Matthew, B. Traffic Energy and Emission Reductions at Signalized Intersections: A Study of the Benefits of Advanced Driver Information. *Int. J. Intell. Transp. Syst. Res.* **2009**, *7*, 2327–2332.
  24. Xia, H.; Boriboonsomsin, K.; Barth, M. Indirect network-wide energy/emissions benefits from dynamic eco-driving on signalized corridors. In Proceedings of the International IEEE Conference on Intelligent Transportation Systems, Washington, DC, USA, 5–7 October 2011; pp. 329–334. [[CrossRef](#)]
  25. Xia, H.; Wu, G.; Boriboonsomsin, K.; Barth, M. Development and evaluation of an enhanced eco-approach traffic signal application for Connected Vehicles. In Proceedings of the International IEEE Conference on Intelligent Transportation Systems, The Hague, The Netherlands, 6–9 October 2013; pp. 296–301. [[CrossRef](#)]
  26. Xia, H.; Boriboonsomsin, K.; Barth, M. Dynamic Eco-Driving for Signalized Arterial Corridors and Its Indirect Network-Wide Energy/Emissions Benefits. *J. Intell. Transp. Syst.* **2013**, *17*, 31–41. [[CrossRef](#)]
  27. Kamal, M.; Mukai, M.; Murata, J. On board eco-driving system for varying road-traffic environments using model predictive control. *IEEE Int. Conf. Control Appl.* **2010**, *58*, 1636–1641. [[CrossRef](#)]
  28. Rakha, H.; Kamalanathsharma, R.K. Eco-driving at signalized intersections using V2I communication. In Proceedings of the International IEEE Conference on Intelligent Transportation Systems, Washington, DC, USA, 5–7 October 2011; pp. 341–346. [[CrossRef](#)]
  29. Mensing, F.; Trigui, R.; Bideaux, E. Vehicle trajectory optimization for application in ECO-driving. In Proceedings of the IEEE Vehicle Power and Propulsion Conference, Chicago, IL, USA, 6–9 September 2011; pp. 1–6. [[CrossRef](#)]
  30. Nunzio, G.; Wit, C.C.; Moulin, P. Eco-driving in urban traffic networks using traffic signals information. *Decis. Control* **2014**, *26*, 1307–1324. [[CrossRef](#)]
  31. Prendinger, H.; Oliveira, J.; Catarino, J. iCO<sub>2</sub>: A Networked Game for Collecting Large-Scale Eco-Driving Behavior Data. *IEEE Internet Comput.* **2014**, *18*, 28–35. [[CrossRef](#)]
  32. Qi, X.; Wu, G.; Boriboonsomsin, K.; Barth, M. Evolutionary algorithm based on-line PHEV energy management system with self-adaptive SOC control. In Proceedings of the Intelligent Vehicles Symposium, Seoul, Korea, 28 June–1 July 2015; pp. 425–430. [[CrossRef](#)]
  33. He, X.; Liu, H.X.; Liu, X. Optimal vehicle speed trajectory on a signalized arterial with consideration of queue. *Transp. Res. Part C* **2015**, *61*, 106–120. [[CrossRef](#)]
  34. Yang, H.; Rakha, H.; Ala, M.V. Eco-Cooperative Adaptive Cruise Control at Signalized Intersections Considering Queue Effects. *IEEE Trans. Intell. Transp. Syst.* **2017**, *18*, 1575–1585. [[CrossRef](#)]
  35. Jiang, H.; Hu, J.; An, S.; Wang, M.; Park, B.B. Eco approaching at an isolated signalized intersection under partially connected and automated vehicles environment. *Transp. Res. Part C* **2017**, *79*, 290–307. [[CrossRef](#)]
  36. Zohdy, I.A.; Rakha, H.A. Intersection management via vehicle connectivity: The intersection cooperative adaptive cruise control system concept. *J. Intell. Transp. Syst.* **2016**, *20*, 17–32. [[CrossRef](#)]
  37. Huang, X.; Peng, H. Speed trajectory planning at signalized intersections using sequential convex optimization. In Proceedings of the American Control Conference (ACC), Seattle, WA, USA, 24–26 May 2017; pp. 2992–2997. [[CrossRef](#)]
  38. Hao, P.; Wu, G.; Boriboonsomsin, K.; Barth, M. Developing a framework of eco-approach and departure application for actuated signal control. In Proceedings of the Intelligent Vehicles Symposium (IV), Seoul, Korea, 28 June–1 July 2017; pp. 796–801. [[CrossRef](#)]
  39. Xia, H. Eco-Approach and Departure Techniques for Connected Vehicles at Signalized Traffic Intersections. Ph.D. Thesis, University of California, Riverside, CA, USA, 2014.
  40. Xiao, L.; Gao, F. Effect of information delay on string stability of platoon of automated vehicles under typical information frameworks. *J. Cent. South Univ. Technol.* **2010**, *17*, 1271–1278. [[CrossRef](#)]
  41. Akcelik, R. Efficiency and drag in the power-based model of fuel consumption. *Transp. Res. Part B* **1989**, *23*, 376–385. [[CrossRef](#)]

